Volume change indices during loading and unloading of an unsaturated soil

D. Y. F. Ho

Geo-environmental Group, EBA Engineering Consultants Ltd., Civil, Geotechnical, and Materials Engineers, Edmonton, Alta., Canada

D. G. Fredlund

Department of Civil Engineering, University of Saskatchewan, Saskatoon, Sask., Canada

AND

H. Rahardjo

School of Civil and Structural Engineering, Nanyang Technological University, Singapore, Singapore

Received January 2, 1991

Accepted December 13, 1991

The paper presents the volume change theory and the designation of associated soil properties that must be measured for an unsaturated soil. The equipment required for the measurement of each of the relevant volume relationships is described. Several testing procedures for obtaining the volume change indices during loading and unloading of an unsaturated soil are presented. Typical results from loading and unloading tests on compacted silt and compacted glacial till specimens are presented and analyzed. The analysis is given in order to illustrate the application of the volume change theory to practical problems.

Key words: unsaturated soil, volume change indices, constitutive relations, coefficients of volume change, oedometer tests.

Cet article présente la théorie de changement de volume et l'identification des propriétés associées des sols qui doivent être mesurées pour un sol non saturé. L'équipement requis pour la mesure de chacune des relations de volume appropriées est décrit. Plusieurs procédures d'essais pour obtenir les indices de changement de volume lors du chargement et déchargement d'un sol non saturé sont présentées. Des résultats typiques de chargement et déchargement sur des spécimens de silt compacté et de till glaciaire compacté sont présentés et analysés. L'on présente l'analyse afin d'illustrer l'application à des problèmes pratiques de la théorie de changement de volume.

Mots clés : sol non saturé, indices de changement de volume, relations de comportement, coefficients de changement de volume, essais oedométriques.

[Traduit par la rédaction]

Can. Geotech. J. **29**, 195–207 (1992)

Introduction

Many geotechnical works involve soils with negative pore-water pressures, and often these soils are unsaturated. Natural soils above the groundwater table and compacted soils in roads and earth dams are typical examples of unsaturated soils. Volume changes of the soil due to applied loads or environmental changes (i.e., rainfall and evaporation) are of interest to practising engineers.

The volume change theory and testing procedures for saturated soils are well known to geotechnical engineers. Extensions to the theory and testing procedures are required for the prediction of volume changes in an unsaturated soil. These extensions are presented in the paper. Typical volume changes during loadings and unloadings of unsaturated, compacted silts and glacial tills are presented and analyzed to illustrate the application of the extended theory.

Constitutive relations for an unsaturated soil

In saturated soils, volume changes due to loading are usually presented as a relationship between void ratio e and effective stress (i.e., $\sigma - u_w$, where σ is total normal stress and u_w is pore-water pressure) expressed on a logarithmic scale[1] (Terzaghi 1943). The logarithmic slope of the loading curve is called the compression index C_c, and the logarithmic slope of the unloading curve is called the swell index C_s. The void ratio versus log $(\sigma - u_w)$ relationship is obtained from conventional consolidation tests. The soil volume change associated with the soil structure of a saturated soil is always equal to the water volume change.

In an unsaturated soil, two stress-state variables govern the volume change behaviour; namely, net normal stress $(\sigma - u_a)$, and matric suction $(u_a - u_w)$, where u_a is pore-air pressure. Therefore, the void ratio e must now be related to the $(\sigma - u_a)$ and $(u_a - u_w)$ stress-state variables (Fig. 1). In addition, an independent relationship for the soil water content w (Fig. 2) is required to obtain a complete description of the volume change in an unsaturated soil. These constitutive surfaces are the same as those proposed by Fredlund and Morgenstern (1976). The difference between the soil structure and water volume changes is equal to the air volume change.

Void ratio constitutive surface

The soil structure constitutive surface is a concave, warped surface when plotted on an arithmetic scale. The same surface resembles a quarter section of the convex surface of a vertical cone when plotted on a semilogarithmic scale. A schematic diagram of the soil structure constitutive surfaces for monotonic volume changes is shown in Fig. 1. The intersection curves of the arithmetic surface of void ratio on the $(\sigma - u_a)$ and $(u_a - u_w)$ planes (Fig. 1*a*) result in the

[1]Note that, for simplicity in this paper, variables expressed on a logarithmic scale are indicated as the log of the variables in question, e.g., the effective stress graphed on a logarithmic scale is indicated as log $(\sigma - u_w)$.

Printed in Canada / Imprimé au Canada

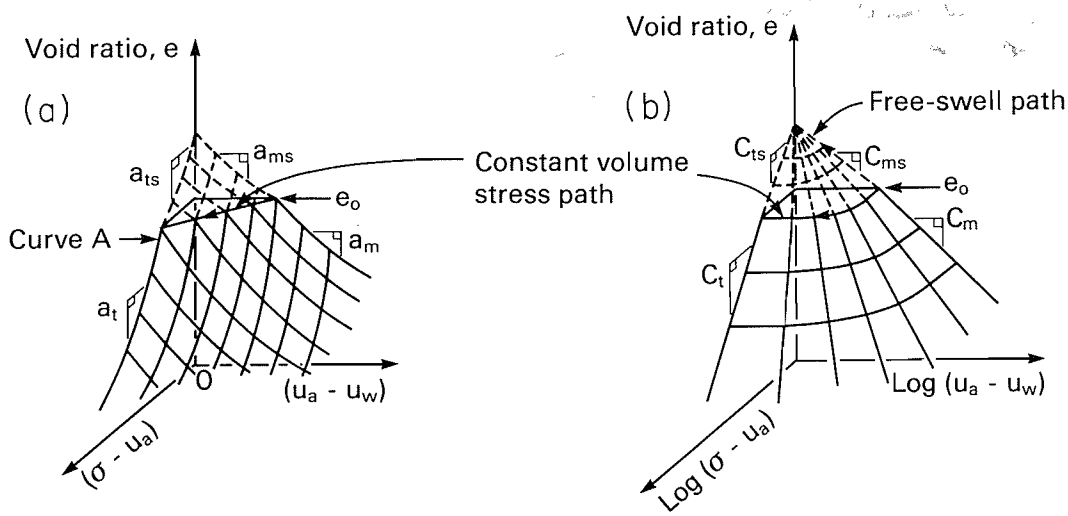

FIG. 1. Proposed soil structure constitutive surfaces for an unsaturated soil. Schematic diagram of the void ratio constitutive surfaces for monotonic volume changes on (*a*) an arithmetic scale and (*b*) a semilogarithmic scale. - - -, swelling or rebound; —, compression.

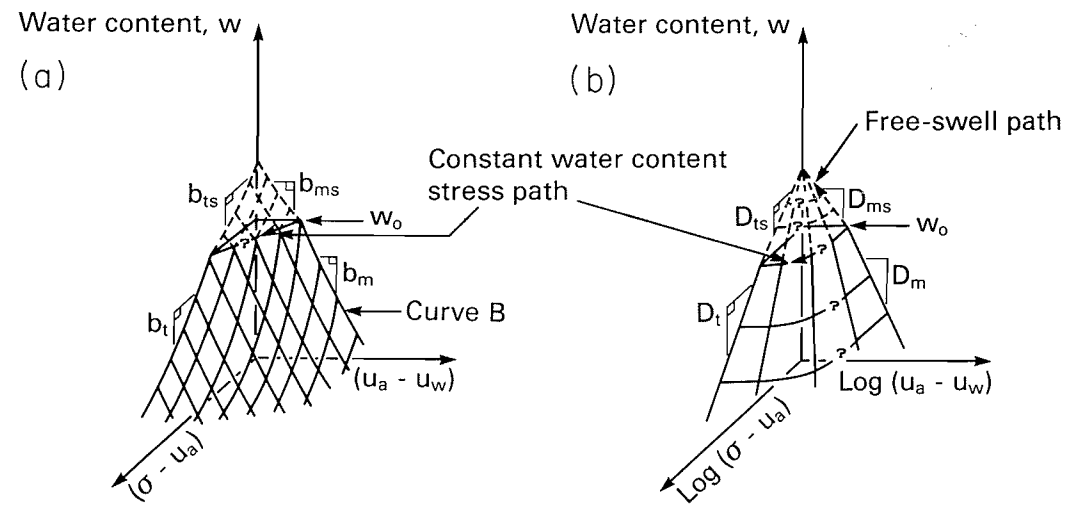

FIG. 2. Proposed water content constitutive surfaces for an unsaturated soil. Schematic diagram of the water content constitutive surfaces for monotonic volume changes on (*a*) an arithmetic scale and (*b*) a semilogarithmic scale. - - -, water content increase; —, water content decrease.

definition of four compressibility coefficients (i.e., a_t, a_{ts}, a_m, and a_{ms}) where a_t and a_{ts} are coefficients of compressibility and swelling with respect to the net normal stress for monotonic volume decrease and increase, respectively, and a_m and a_{ms} are coefficients of compressibility and swelling with respect to the matric suction for monotonic volume decrease and increase, respectively.

The shape of the intersection curve on the $(\sigma - u_a)$ plane is well established when matric suction is equal to zero (i.e., e vs. $(\sigma - u_w)$ curve). This curve is the same as the conventional consolidation curve for a saturated soil. A typical compression of a natural, saturated soil consists of recompression and virgin compression branches (Terzaghi and Peck 1967). The virgin compression curve is exponential on an arithmetic scale and can be linearized on a semilogarithmic plot. The rebound curves are approximately parallel to one another and can be linearized on a semilogarithmic scale (Schmertmann 1955; Holtz and Gibbs 1956; Gilchrist 1963; Noble 1966; Lambe and Whitman 1979; Lidgren 1970; Chen 1975).

Soils can be overconsolidated by desiccation and rebounded due to a suction decrease. The virgin compression branch and rebound curves are essentially linear on a semilogarithmic scale (Fredlund 1967; Aitchison and Woodburn 1969; Escario 1969; Aitchison and Martin 1973; Richards *et al.* 1984). There are pressure range limits that must be kept to ensure linearity. A constant volume (i.e., constant void ratio) stress path, where an unsaturated soil is moving towards saturation, is essentially a straight line on an arithmetic plot of the stress-state variables (Escario 1969). The same path becomes a convex asymptotic curve on a logarithmic scale.

Water phase constitutive surface

There is insufficient information in the literature to definitely define the form of the water phase constitutive surface. The water content and void ratio constitutive relations are interrelated by the specific gravity G_s when a soil is saturated (i.e., $e = wG_s$ when $S = 100\%$). Conclusions arrived at for the void ratio constitutive relation are also assumed to apply to the water phase constitutive relation.

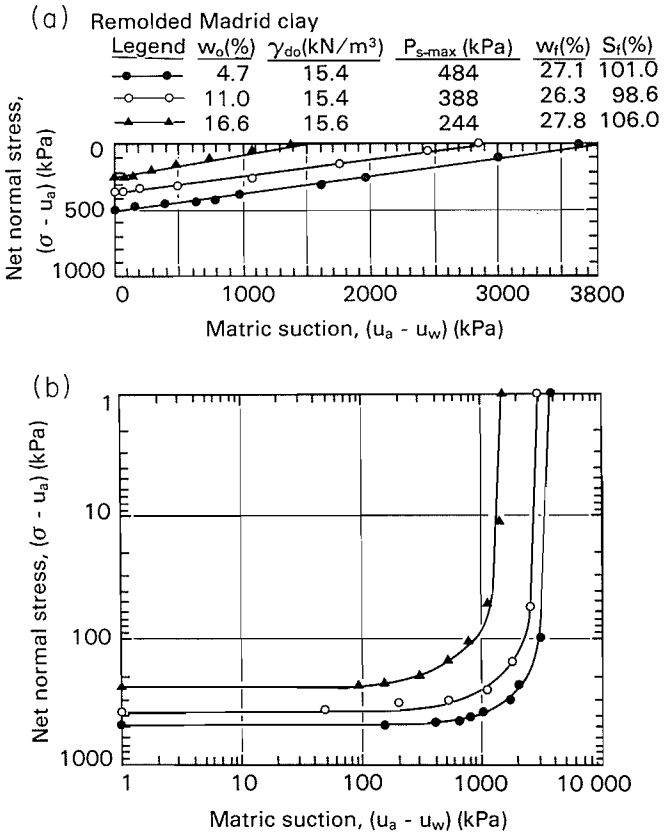

FIG. 3. Cross sections of void ratio surfaces plotted on (a) ($\sigma - u_a$) and ($u_a - u_w$) planes (arithmetic scale) and (b) log ($\sigma - u_a$) and log ($u_a - u_w$) planes (logarithmic scale) (modified from Escario 1969).

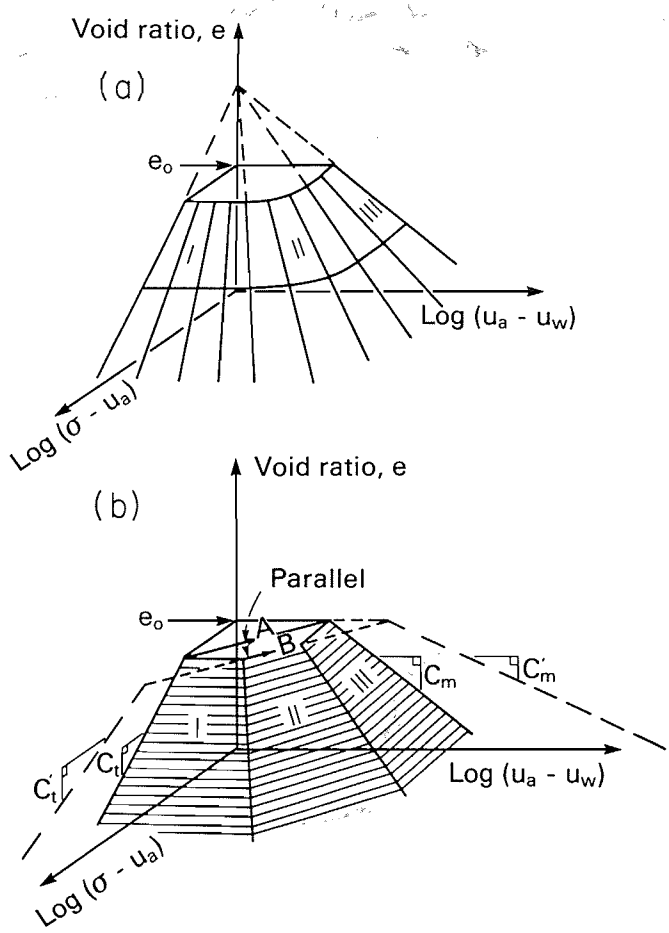

FIG. 4. Logarithmic forms of void ratio constitutive surface for loading conditions (from Ho 1988). (a) Void ratio constitutive surface for loading as plotted logarithmically. (b) Approximated form of the void ratio constitutive surface in the logarithmic plot.

There is evidence that the water content versus matric suction constitutive curves on a semilogarithmic scale are essentially linear when the net normal stress is equal to zero (Croney and Coleman 1954; Fredlund 1967; McWhorter and Nelson 1979; Mitchell and Avalle 1984). Once again, there are pressure limits within which there is linearity. The same curves are therefore approximately exponential on arithmetic plots.

There is no known experimental information available on the shape of a constant water content stress path on the constitutive surface. When a soil approaches saturation, a change in net normal stress becomes as effective as a change in matric suction in changing the water content. A constant water content stress path must therefore approach a 45° line when the matric suction tends to zero. This angle forms an upper limit. A constant water content stress path on the water phase constitutive surface will be assumed to be a straight line on an arithmetic plot of water content versus net normal stress and matric suction (Fig. 2a). The resulting constitutive surface is a concave surface when water content is increased or decreased. The same surface resembles a quarter section of the convex surface of a vertical cone on a water content versus the logarithm of net normal stress and matric suction.

A schematic diagram of the water phase constitutive surfaces for monotonic volume changes is presented in Fig. 2. The intersection curves of the arithmetic surface of water content on the ($\sigma - u_a$) and ($u_a - u_w$) planes (Fig. 2a) result in four coefficients of water change, namely b_t, b_{ts}, b_m, and b_{ms}, where b_t and b_{ts} are coefficient of water content change and rebound coefficient of water content change with respect to the net normal stress for monotonic water content decrease and increase, respectively; and b_m and b_{ms} are coefficient of water content change and rebound coefficient of water content change with respect to the matric suction for monotonic water content decrease and increase, respectively.

The above volumetric deformation coefficients vary from one state point to another along a nonlinear constitutive surface. A direct method to determine these coefficients at a specific state point is to measure their magnitude at the stress point under consideration. The experimental measurements required are similar to those conducted for the verification of the constitutive surfaces. It may require numerous specimens and a long period of testing if the entire constitutive surface is to be defined.

A simpler procedure would be to assume that the constitutive surface is planar at a particular void ratio or water content. Therefore, every point on the surface corresponding to an equal void ratio or water content plane would have the same a_t and a_m coefficients or b_t and b_m coefficients, respectively. As a result, the a_t and b_t coefficients obtained from the saturation plane (i.e., ($u_a - u_w$) equal to zero plane) can be used for other points on the surface as long as the void ratio (or water content) is constant. Similarly, the a_m and b_m coefficients obtained from the zero net nor-

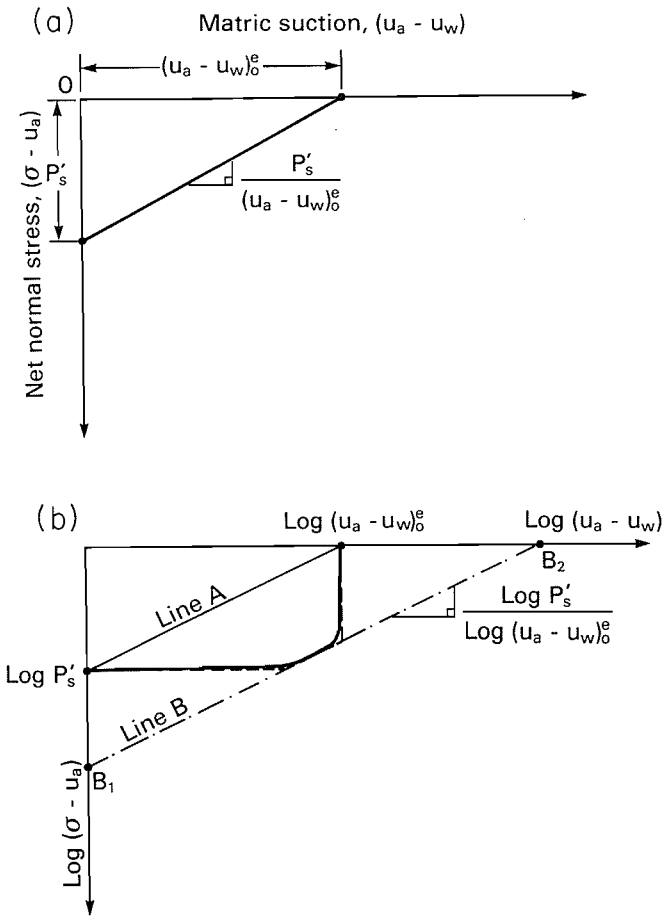

FIG. 5. Construction of lines A and B from constant-volume oedometer test results. Constant-volume stress path on (*a*) an arithmetic scale and (*b*) a logarithmic scale. P'_s, corrected swelling pressure; $(u_a - u_w)^e_o$, matric suction corresponding to zero net normal stress at a constant void ratio. —, actual stress path; - - -, approximate stress path.

mal stress plane (i.e., $(\sigma - u_a)$ equal to zero plane) can also be used for other points on the surface along a constant void ratio or water content plane. In other words, the values of a_t, a_m, b_t, and b_m obtained on the saturation and zero net normal stress planes can be used for the entire constitutive surface.

The above method of determination of the volumetric coefficients is much simpler than defining the entire constitutive surface. However, it may be inferior to the use of the direct determination of volume change coefficients obtained at individual state points. The applicability of this approach will depend primarily on the character of the constitutive surfaces as established through laboratory experiments and on the reliability required in an analysis. The required level of accuracy in solving a problem must also be borne in mind when using the above assumption. In general, the suggested procedure may be sufficiently accurate for many geotechnical applications.

Semilogarithmic forms of constitutive surfaces

The logarithmic plots of constitutive surfaces (Figs. 1*b* and 2*b*) exhibit linear curves on the extreme planes (i.e., the plane with log $(u_a - u_w)$ approximately equal to 0 and the plane with log $(\sigma - u_a)$ approximately equal to 0). The slopes of the curves on these extreme planes are called indices. The volumetric deformation indices associated with the void ratio surface (Fig. 1*b*) are C_t, C_{ts}, C_m, and C_{ms}, where C_t and C_{ts} are compressive and swelling indices with respect to the net normal stress for monotonic volume decrease and increase, respectively; and C_m and C_{ms} are compressive and swelling indices with respect to the matric suction for monotonic volume decrease and increase, respectively.

The volumetric deformation indices associated with the water phase surface (Fig. 2*b*) are D_t, D_{ts}, D_m, and D_{ms}, where D_t and D_{ts} are water content and rebound water content indices with respect to the net normal stress for monotonic water content decrease and increase, respectively; and D_m and D_{ms} are water content and rebound water content indices with respect to the matric suction for monotonic water content decrease and increase, respectively.

The C_t, C_m, D_t, and D_m indices can be obtained from the same test data used to obtain the a_t, a_m, b_t, and b_m coefficients. The difference is in the manner in which the results are plotted. Using a conversion between a semilogarithmic and an arithmetic scale (Lambe and Whitman 1979), the C_t, C_m, D_t, and D_m indices can be written in terms of the a_t, a_m, b_t, and b_m coefficients.

$$[1] \quad C_t = \frac{a_t(\sigma - u_a)_{ave}}{0.435}$$

$$[2] \quad C_m = \frac{a_m(u_a - u_w)_{ave}}{0.435}$$

$$[3] \quad D_t = \frac{b_t(\sigma - u_a)_{ave}}{0.435}$$

$$[4] \quad D_m = \frac{b_m(u_a - u_w)_{ave}}{0.435}$$

where $(\sigma - u_a)_{ave}$ is the average of the initial and final net normal stresses for an increment, and $(u_a - u_w)_{ave}$ is the average of the initial and final matric suctions for an increment.

Despite the linear curves on the extreme planes, the cross section of the constitutive surface on the log $(\sigma - u_a)$ and log $(u_a - u_w)$ planes is no longer a series of straight lines as are found on the $(\sigma - u_a)$ and $(u_a - u_w)$ planes. Figure 3 shows a comparison of the constitutive surface cross section at a constant void ratio when plotted using the arithmetic and logarithmic scales. An essentially linear cross section on the arithmetic plot becomes an asymptotic curve on the logarithmic plot.

The asymptotic cross-section curve suggests the logarithmic form of the void ratio constitutive surface as illustrated in Fig. 4*a*. An approximated form of the void ratio constitutive surface can be used in the analysis as shown in Fig. 4*b*. The approximated surface consists of three planes, namely planes I, II, and III. The three planes converge at a void ratio ordinate corresponding to nominal values of the stress-state variables (i.e., log $(\sigma - u_a) \approx 0$ and log $(u_a - u_w) \approx 0$). Planes I and III are referred to as the orthogonal planes. Plane I is perpendicular to the void ratio versus log $(\sigma - u_a)$ plane, and the slope of plane I gives the C_t index. Plane III is perpendicular to the void ratio versus log $(u_a - u_w)$ plane, and the slope of plane III gives the C_m index. In other words, only one index is required to describe the void ratio changes when the stress-state variable changes occur within the regions defined by planes I and III. There-

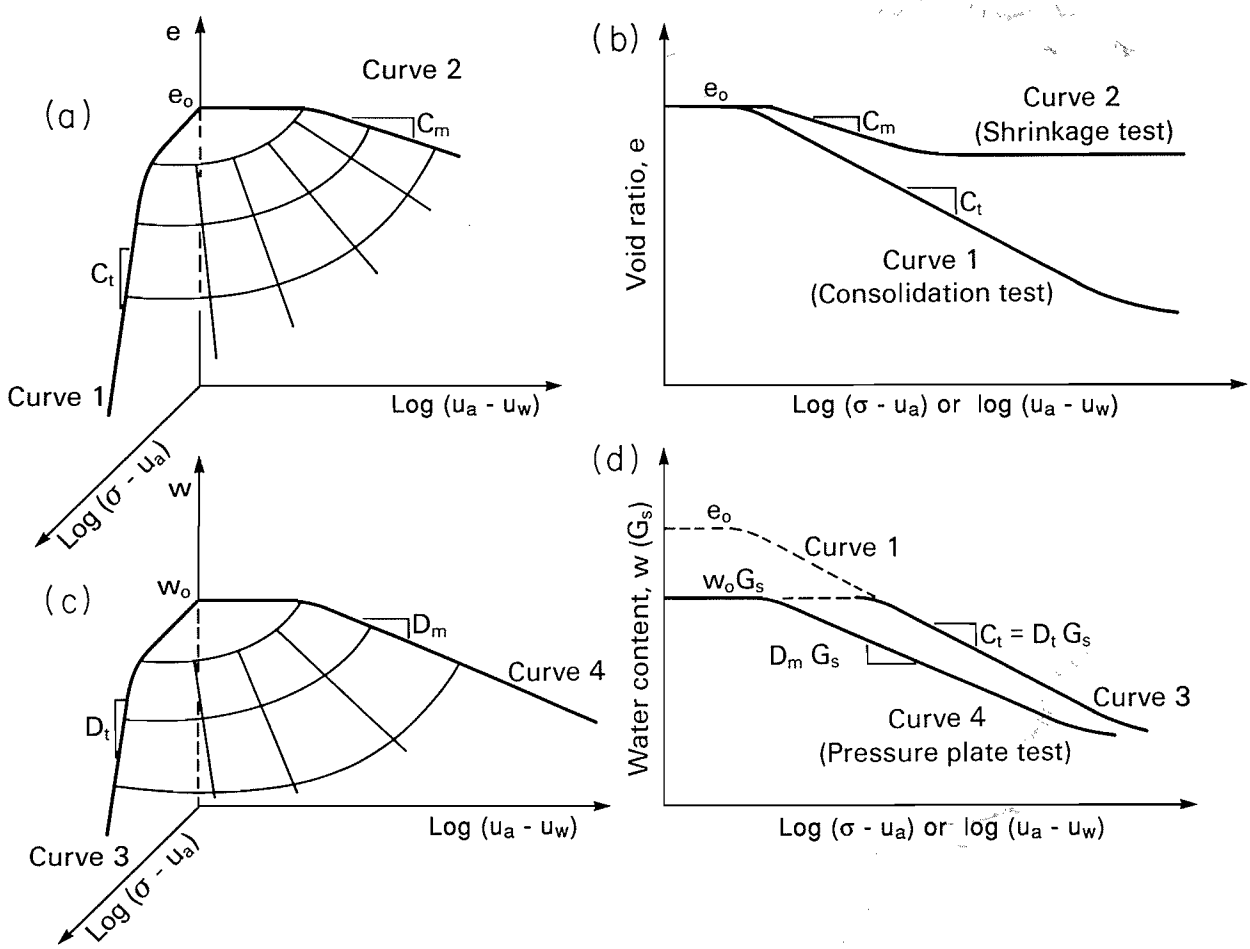

FIG. 6. Void ratio and water content relationship for an unsaturated soil. (*a*) Void ratio relationship. (*b*) Intersection curves between void ratio surface and log ($\sigma - u_a$) or log ($u_a - u_w$) plane. (*c*) Water content relationship. (*d*) Intersection curves between water content surface and log ($\sigma - u_a$) or log ($u_a - u_w$) plane.

fore, the constitutive equation describing plane I can be written as

$$[5] \quad de = C_t \, d[\log (\sigma - u_a)]$$

and the equation for plane III is as follows:

$$[6] \quad de = C_m \, d[\log (u_a - u_w)]$$

Plane II represents a transition zone between planes I and III. This plane intersects both the void ratio versus log ($\sigma - u_a$) plane and the void ratio versus log ($u_a - u_w$) plane. The slopes of the intersection lines define the slopes of plane II, namely the C_t' and C_m' indices. In this case, two indices are required to describe void ratio changes when the stress-state variable changes occur within in the region of plane II. The constitutive equation describing plane II can be written as

$$[7] \quad de = C_t' \, d[\log (\sigma - u_a)] + C_m' \, d[\log (u_a - u_w)]$$

where C_t' is the slope of the intersection line of plane II with the e versus log ($\sigma - u_a$) plane, and C_m' is the slope of the intersection line of plane II with the e versus log ($u_a - u_w$) plane.

It should also be noted that line B associated with plane II is assumed to be parallel to line A which joins planes I and III (Fig. 4*b*). This assumption is required in constructing the intersection lines of plane II on the extreme planes as illustrated in Fig. 5. Line B intersects the extreme planes at points B_1 and B_2. The lines joining the intersection points B_1 and B_2 to the convergence void ratio ordinate gives the C_t' and C_m' indices, respectively.

Unloading constitutive surfaces

The above approximation is also applicable to the unloading surface of void ratio (Ho 1988). The shape of the water content constitutive surface is not fully understood. It is a matter of speculation to assume that the water content constitutive surface is similar in shape to the void ratio constitutive surface. However, there does not appear to be any experimental data to substantiate this assumption.

Relationships between volume change indices

The relationships between the volume change indices associated with the loading conditions can best be visualized by presenting the intersection curves on one plot (Ho and Fredlund 1989; Rahardjo *et al.* 1990). The intersection curves 1 and 2 from the void ratio surface (Fig. 6*a*) are combined in Fig. 6*b*. The slopes of curves 1 and 2 are called C_t and C_m volume change indices, respectively. The intersection curves 3 and 4 from the water content surface (Fig. 6*c*) are combined in Fig. 6*d*. The water content w can be multiplied by the specific gravity G_s (i.e., wG_s) to make use of the basic volume–mass relationship (i.e., $Se = wG_s$, where S is degree of saturation) in obtaining one of the index relationships. This means that curves 3 and 4 in Fig. 6*c* are trans-

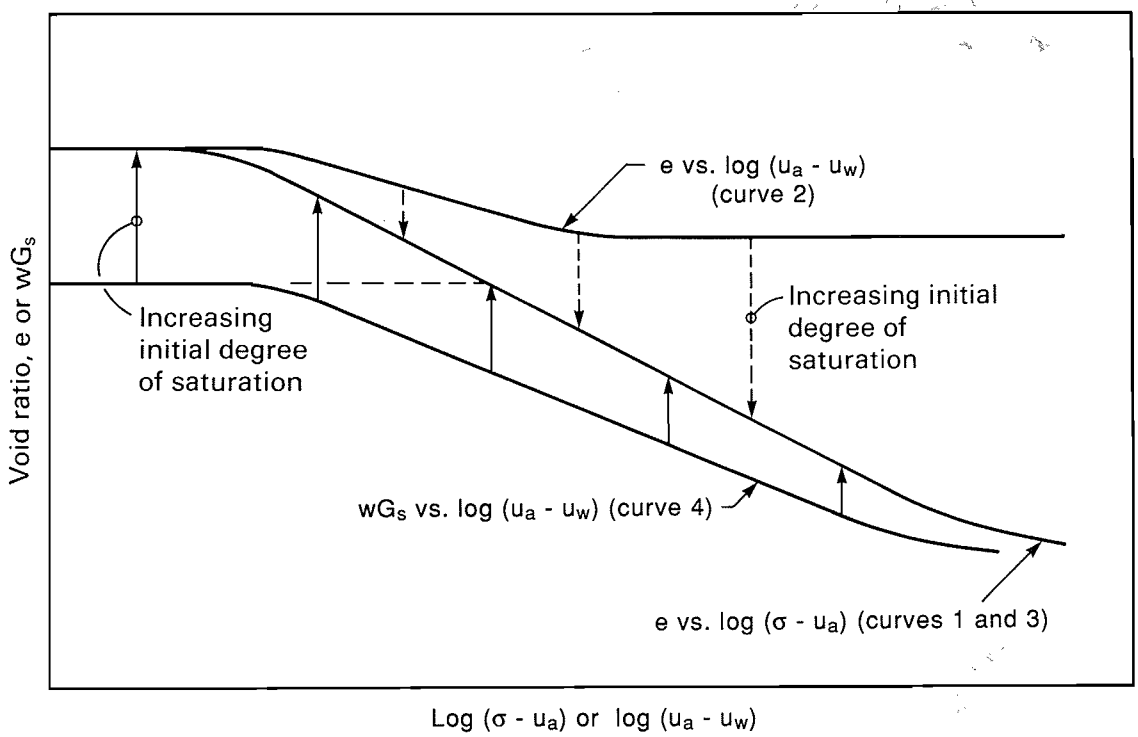

FIG. 7. Relationship between curves that define the volume change behavior of an unsaturated soil.

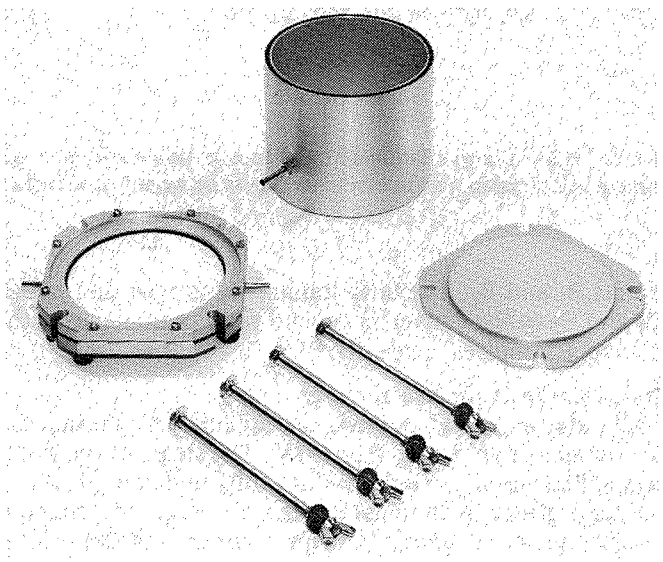

FIG. 8. Volumetric pressure-plate extractor (i.e., maximum applied matric suction is 200 kPa) (photography courtesy of Soilmoisture Equipment Corporation, Santa Barbara, Calif.).

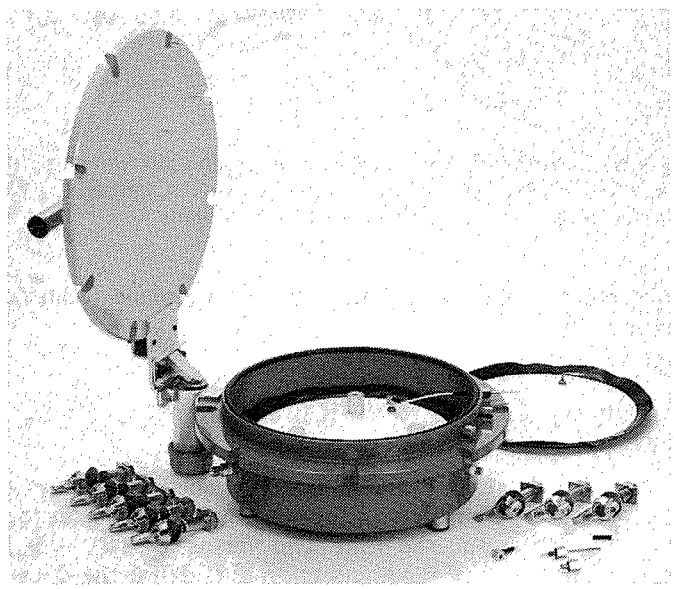

FIG. 9. 15 bar ceramic-plate extractor (i.e., maximum applied matric suction is 1500 (kPa) (photograph courtesy of Soilmoisure Equipment Corporation, Santa Barbara, Calif.).

lated vertically by a magnitude of G_s in Fig. 6*d*. As a result, the slopes of curves 3 and 4 in Fig. 6*d* are the products of G_s and the volume change indices (i.e., $D_t G_s$ and $D_m G_s$, respectively).

Curve 1 in Fig. 6 is essentially the consolidation curve for the soil in a saturated condition (i.e., $u_a - u_w = 0$, or $u_a = u_w$). The curve exhibits a linear relationship between void ratio and the logarithmic scale of net normal stress, over a wide loading range. The slope of curve 1, C_t, is equal to the compression index C_c of the saturated soil. Curve 3 in Fig. 6*d* coincides with curve 1 from Fig. 6*b*, since wG_s is equal to the void ratio when the soil is saturated (i.e., $S = 1$). Therefore, the water content index D_t can be computed as C_t/G_s.

Curve 4 in Fig. 6 is called a soil-water characteristic curve that can be obtained from a pressure-plate test (see Test procedures and equipment). A shrinkage test curve combined with the soil-water characteristic curve can be used to construct curve 2 in Fig. 6. In other words, the four volume change curves and their corresponding indices (i.e., C_t, D_t, D_m, and C_m) can be obtained from routine soil tests.

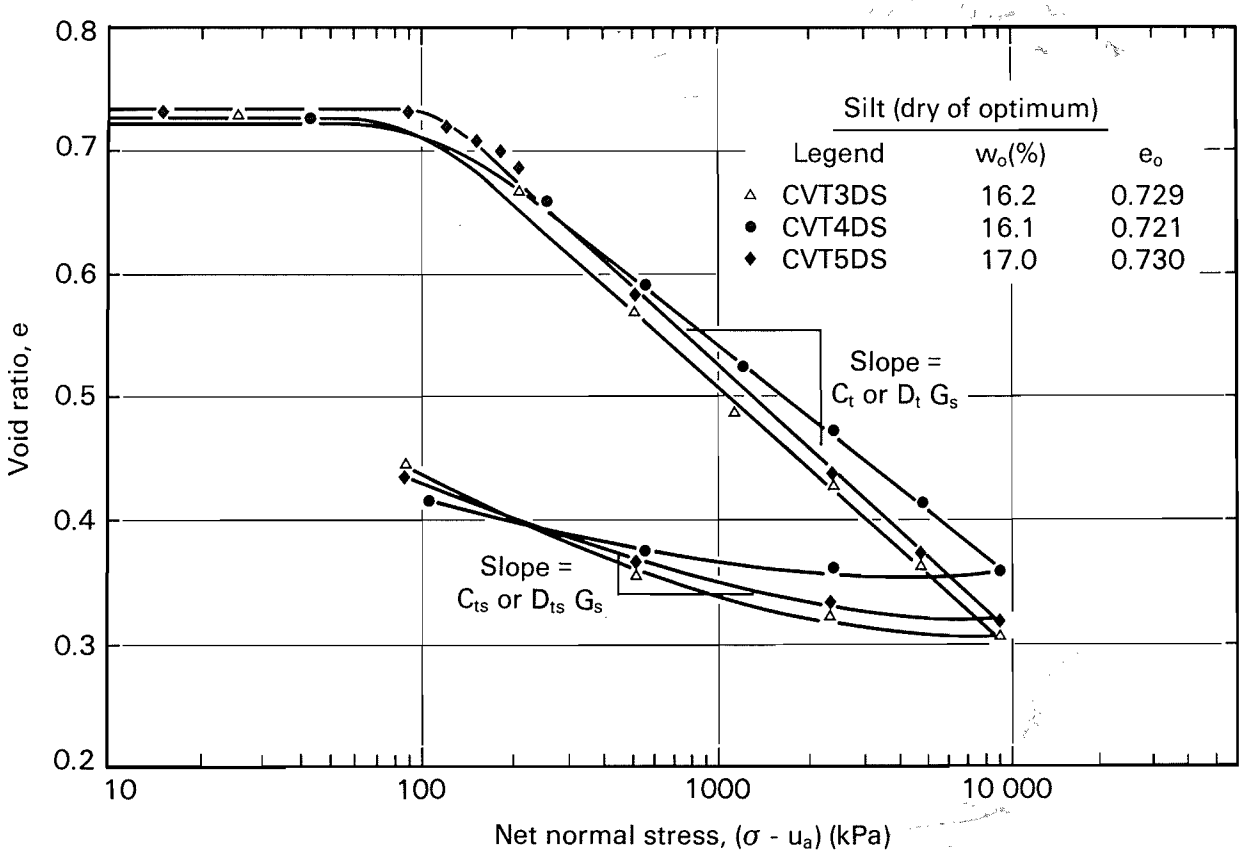

FIG. 10. Results from one-dimensional constant volume tests on a compacted silt.

The combined plot of curves 1, 2, 3, and 4 is presented in Fig. 7, which is essentially a combination of Figs. 6*b* and 6*d*. The arrows in Fig. 7 indicate the direction of curves 2 and 4 approaching curve 1 as the initial degree of saturation of the soil increases. In this case, curve 1 is assumed to remain constant for various initial degrees of saturation. When the soil is saturated (i.e., $u_a - u_w = 0$, or $u_a = u_w$), the void ratio and wG_s vary only with respect to net normal stress or the effective stress ($\sigma - u_w$) following the same curve (i.e., curve 1 in Fig. 7).

The volume change indices pertinent to the unloading conditions can be obtained from the unloading portion of the consolidation curve and the free-swell test. Unloading curves with respect to the net normal stress ($\sigma - u_a$) are approximately parallel to one another (Lambe and Whitman 1979). Therefore, the unloading curve established at the end of the loading sequence can also be considered as the unloading curve of the specimen from its initial state. The slope of the unloading curve from the conventional consolidation test is commonly referred to as the swell index C_s, which can be considered to be equal to the C_{ts} index. Similar to the loading conditions, the rebound water content index D_{ts} can be computed as C_{ts}/G_s.

The C_{ms} and D_{ms} indices are obtained from the free-swell test where the soil specimen undergoes a wetting process under a nominal applied load (i.e., $\sigma - u_a$). The soil matric suction ($u_a - u_w$) is reduced to a nominal magnitude at the end of the test. The state path followed during the free-swell test is indicated in Figs. 1 and 2. Measurements of void ratio and water content changes during the free-swell test allow the determination of the C_{ms} and D_{ms} indices, respectively.

TABLE 1. Index properties of the silt and glacial till used in the test program

	Silt	Glacial till
Liquid limit (%)	26.7	33.2
Plastic limit (%)	14.9	13.0
Plasticity index (%)	11.8	20.2
Percent sand sizes	25.0	32.0
Percent silt sizes	52.0	39.0
Percent clay sizes	23.0	29.0
Specific gravity, G_s	2.72	2.76
Half-standard AASHTO compaction		
$w_{opt.}$ (%)	19.0	18.75
$\gamma_{d\ max.}$ (kN/m^3)	16.65	17.12

Test procedures and equipment

In addition to conventional oedometer tests, there are two other tests required for obtaining the volume change indices for an unsaturated soil. The other two tests are referred to as the pressure-plate test and the shrinkage test.

Oedometer tests

The procedures for performing oedometer tests on unsaturated soil specimens (e.g., compacted specimens) are outlined in ASTM D4546 (ASTM 1985*c*). This ASTM standard describes three methods for inundating the soil specimen prior to performing the compression test. During inundation, the soil matric suction is brought to zero, and the results can be used to calculate the swelling potential of the soil. The inundation can be conducted under either constant-

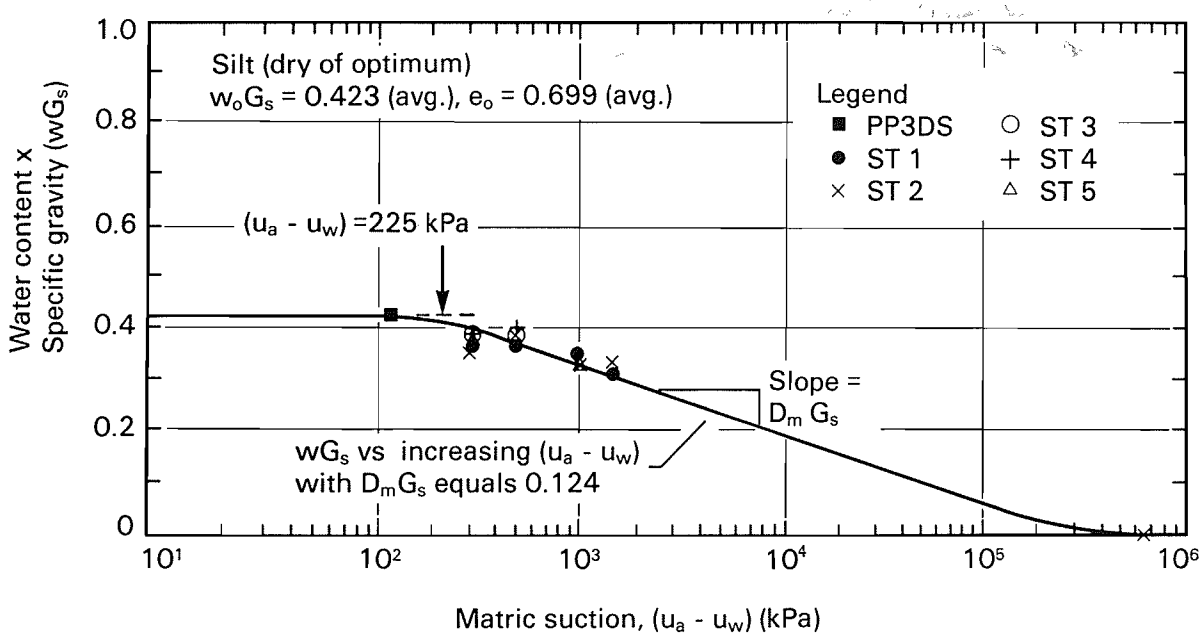

FIG. 11. Soil-water characteristic curve of a compacted silt.

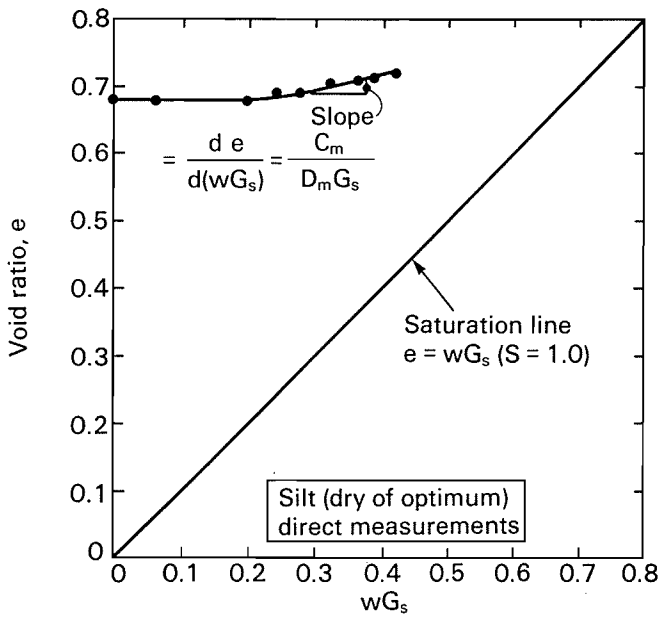

FIG. 12. Shrinkage curve for the compacted silt. Initial conditions: e_0 = 0.720; w_0 = 15.42%.

volume or free-swell conditions. The test can be performed using regular consolidometers.

Curve 1 in Figs. 6 and 7 illustrates the oedometer test results with constant-volume inundation at the beginning of the test. Having inundated the soil specimen, the test can proceed using the conventional procedure used for saturated specimens (ASTM D2435, ASTM 1985*b*). The decreasing void ratios are plotted against the logarithmic scale of effective stress $(\sigma - u_w)$ to yield curves 1 and 3 as shown in Figs. 6 and 7.

At the end of the loading process, the soil specimen can be unloaded with respect to the net normal stress. The increasing void ratios are plotted against the logarithmic scale of effective stress $(\sigma - u_w)$ to yield the rebound curve with a slope equal to C_{ts} or $D_{ts}G_s$.

The void ratio versus log $(u_a - u_w)$ curves at a nominal value of log $(\sigma - u_a)$ are established by conducting the free-swell inundation with void ratio and water content measurements. In this case, more specialized equipment, such as a modified Anteus consolidometer for the K_0-loading condition, is required. The modified Anteus consolidometer allows the control of total, pore-air, and pore-water pressures and the measurements of total and water volume changes during the tests. The soil specimen can be wetted by injecting water through hypodermic needles installed in the loading cap. This procedure was found to be faster than introducing water to the specimen through the high air entry disc at the base of the specimen (Ho 1988).

Pressure-plate tests

The soil-water characteristic curve (i.e., curve 4 in Figs. 6 and 7) of a soil relates the water content to the applied matric suction in the soil. In an unsaturated soil, the pore-air pressure is usually atmospheric (i.e., $u_a = 0$) and the pore-water pressure is negative. The difference in pressures is called the soil matric suction $(u_a - u_w)$. In the laboratory, a matric suction is commonly applied to a soil specimen by maintaining a zero pore-water pressure (i.e., $u_w = 0$) and applying a positive pore-air pressure. Therefore, the matric suction in the soil specimen (i.e., $u_a - u_w$, where u_w is maintained at zero pressure in the compartment below a high air entry disc) can be varied by applying different air pressures to the specimen. This procedure is referred to as the axis-translation technique (Hilf 1956).

Pressure-plate extractors (Soilmoisture Equipment Corporation, Santa Barbara, Calif.) are used to establish the soil-water characteristic curve, and the equipment is shown in Figs. 8 and 9. The extractors are commonly used to apply the various matric suctions to the soil specimen, and the test is called a pressure-plate test (ASTM D2325-68, ASTM 1981). The pressure-plate extractor consists of a high air entry ceramic disc contained in an air pressure chamber. The high air entry disc is saturated and always in contact with water in a compartment below the disc which is maintained at zero water pressure.

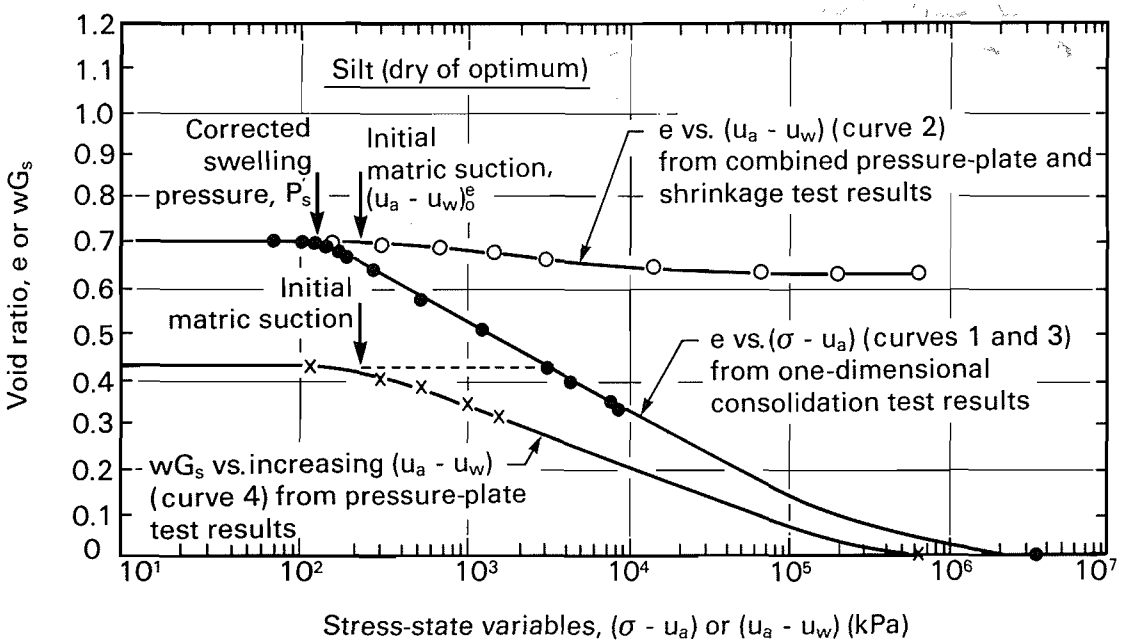

FIG. 13. Volume change relationships for an unsaturated, compacted silt. Average initial condition: $G_s = 2.72$, $e_0 = 0.699$, $w_0 = 15.5\%$, $w_0G_s = 0.420$.

TABLE 2. A summary of the experimentally measured volumetric deformation indices

	One-dimensional loading							One-dimensional unloading					
Soil type	w_0G_s	e_0	C_t or D_tG_s	C_t'	C_m	C_m'	D_mG_s	w_0G_s	e_0	C_{ts}	$D_{ts}G_s$	C_{ms}	$D_{ms}G_s$
DS	0.420	0.699	0.196	0.155	0.030	0.023	0.124	0.419	0.702	0.040	0.126	0.033	0.263
DS	0.424	0.700						0.421	0.699				
OS	0.516	0.606	0.177	0.140	0.082	0.064	0.158	0.517	0.616	0.055	0.076	0.052	0.101
OS	0.511	0.609						0.514	0.609				
DT	0.427	0.642	0.206	0.162	0.089	0.066	0.159	0.436	0.693	0.066	0.084	0.056	0.122
OT	0.516	0.567	0.179	0.137	0.106	0.078	0.171	0.523	0.571	0.037	0.057	0.024	0.060

NOTE: All indices are negative, since an increase in stress-state variable causes a decrease in volume. Soil types: DS, silt at dry of optimum initial water content; OS, silt at optimum initial water content; DT, till at dry of optimum initial water content; OT, till at optimum initial water content. C_{ts} is the average slope of the unloading curve and D_{ts} was calculated from the slope of the linear portion of the unloading curve.

A soil specimen is placed on top of the disc, and the air-tight chamber is pressurized to a desired matric suction. The disc does not allow the passage of air as long as the applied matric suction does not exceed the air-entry value of the disc. This air-entry value is related to the diameter of the fine pores in the ceramic disc. Therefore, the air-entry value of the disc controls the maximum air pressure or matric suction that can be applied to the specimen.

The application of matric suction to the soil causes the pore water to drain to the water compartment through the disc. A burette can be connected to the compartment to measure the water volume changes. At equilibrium, the soil will have a reduced water content corresponding to the increased matric suction. The water content can also be computed at each equilibrium condition from the water volume change measurements if only one specimen is being tested. If more than one specimen is being tested, it is necessary to dismantle the chamber and measure the weight of the specimen at each applied pressure. This procedure is commonly used with 5 and 15 bar ceramic plate extractors, when several specimens are tested simultaneously. Plots of the equilibrium water contents versus the logarithms of the corresponding matric suctions give rise to curve 4 in Figs. 6 and 7.

Shrinkage tests

A shrinkage test gives the relationship between the void ratio and the water content for various matric suctions. A soil specimen can either be allowed to dry in the air or it can be subjected to various matric suctions using the pressure-plate extractors. In either case, the void ratio and water content of the specimen can be measured at various equilibrium states. When the specimen is allowed to dry in air, the process should be interrupted at various stages while the sample is covered and allowed to come to equilibrium.

Accurate measurements of void ratio can be performed following the techniques used in the shrinkage limit test (ASTM D427, ASTM 1985*a*). The shrinkage test involves the measurements of the total volume of the soil specimen using either direct measurements or the mercury-displacement technique. Using the mercury-displacement technique, the

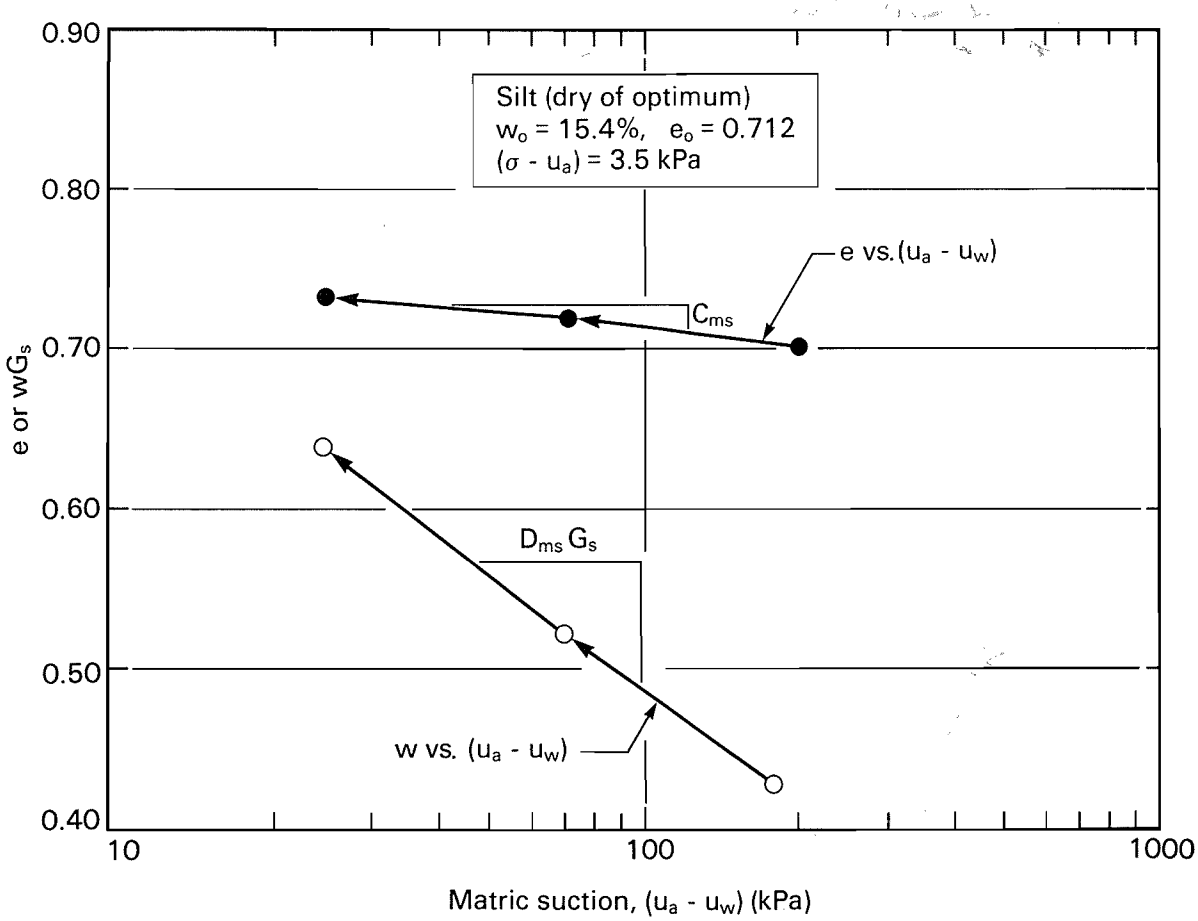

FIG. 14. Results from one-dimensional free-swell test on a compacted silt.

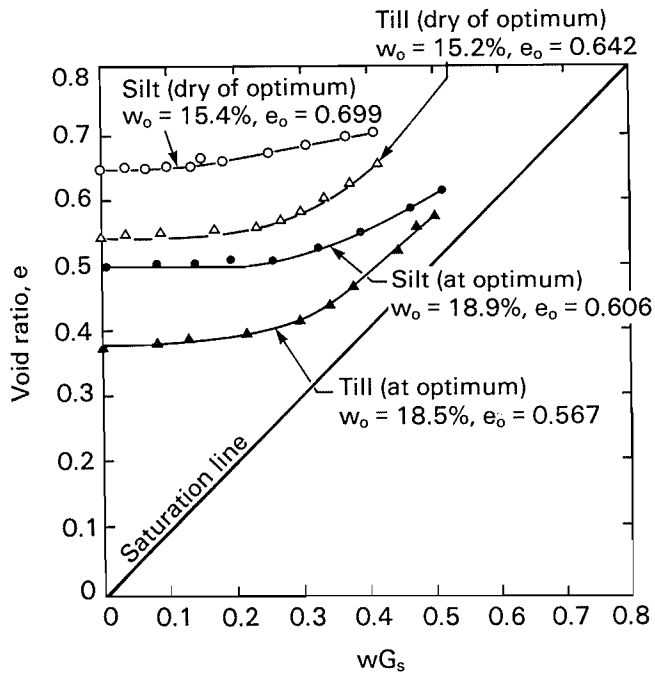

FIG. 15. Shrinkage curves for compacted silt and glacial tills.

volume of the displaced mercury during immersion is equal to the total volume of the specimen.

Direct measurements of total volume can be performed using calipers. The shrinkage curve can be constructed by plotting the void ratios against the water contents as the soil matric suction changes. The test is generally performed for the case of increasing matric suction.

A combination of the shrinkage test data and the water content versus matric suction test data can be used to compute the void ratio versus matric suction relationship for a soil.

Laboratory test program

Two soils, a uniform silt and a glacial till, were tested, and their index properties are presented in Table 1. An attempt was made to prepare specimens with near identical initial conditions. Each soil was oven dried and hand mixed with a predetermined quantity of distilled water. The wet soil was placed in a sealed plastic bag and left to cure in a constant humidity and temperature room. The difference in water content between batches of the same soil was controlled to within 0.5%. Specimens were formed by static compaction at one-half standard Proctor compaction effort at either "dry of optimum" or "at optimum" initial water contents. The compaction characteristics of the silt and glacial till are given in Table 1.

Test results and discussion

The above tests were conducted on compacted silt and till specimens with initial properties corresponding to both the "dry of optimum" and "at optimum" conditions. The results are used to determine the volume change indices for the soils at both compaction conditions.

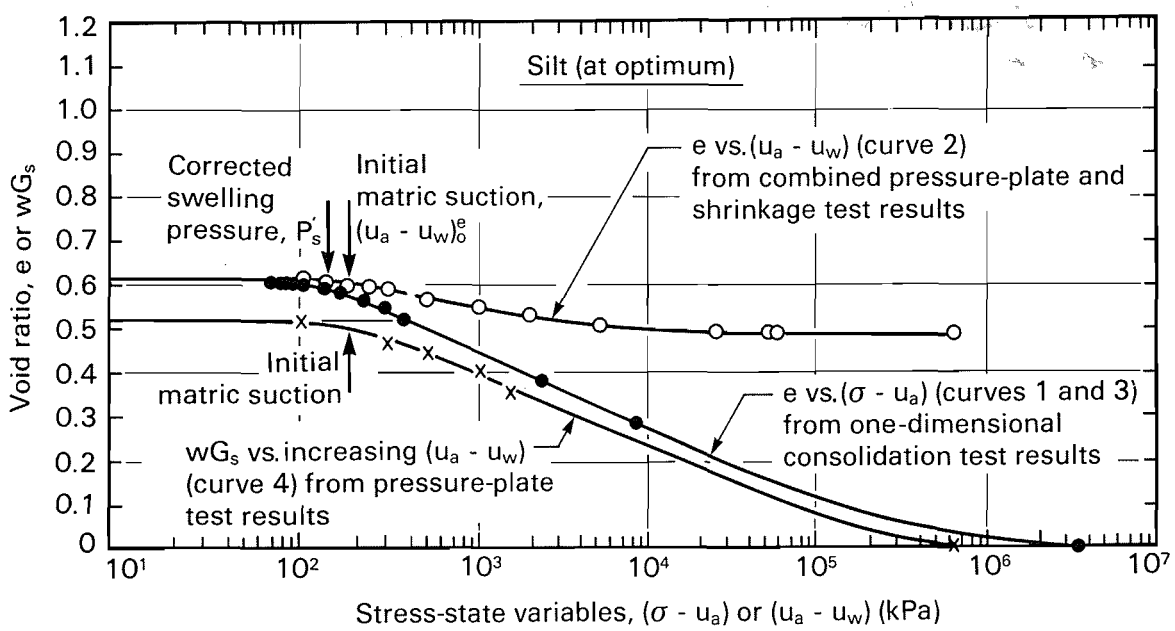

FIG. 16. Volume change relationships for silt at optimum water content under one-dimensional loading conditions. Average initial conditions: $G_s = 2.72$, $e_0 = 0.606$, $w_0 = 19.0\%$, $w_0G_s = 0.516$.

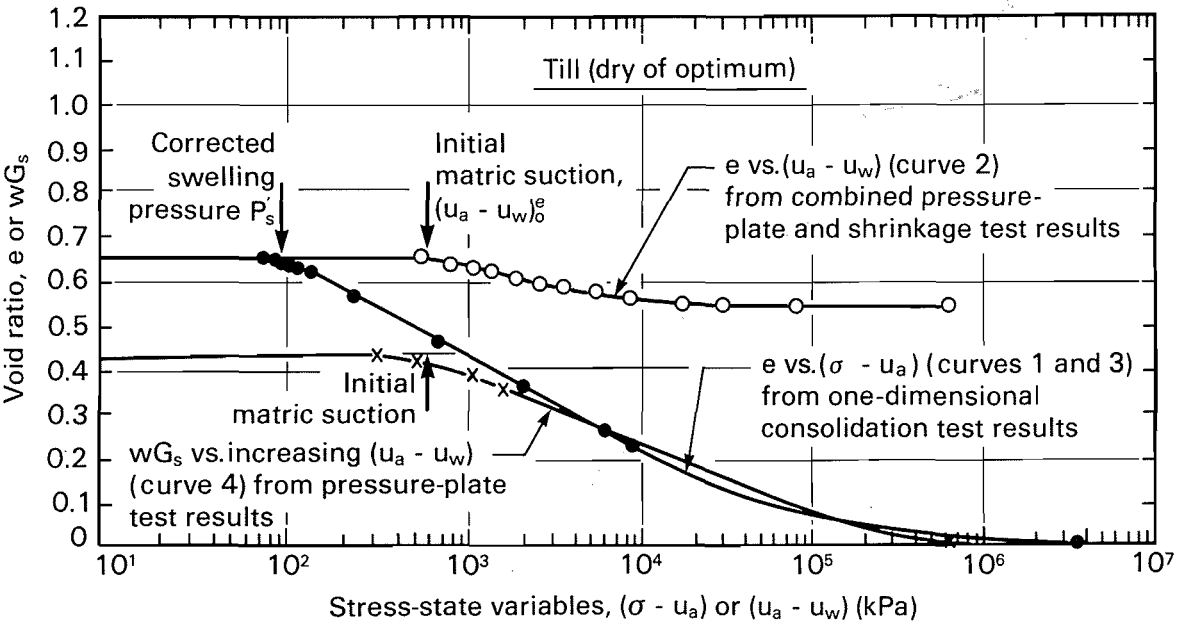

FIG. 17. Volume change relationships for glacial till with dry of optimum water content under one-dimensional loading conditions. Average initial condition: $G_s = 2.76$, $e_0 = 0.642$, $w_0 = 15.4\%$, $w_0G_s = 0.427$.

The set of results from compacted silt specimens at "dry of optimum" condition is used to illustrate the technique for obtaining the volume change indices. The consolidation test results for the silt specimens are shown in Fig. 10. The consolidation tests were performed in accordance with the constant volume test method. The loading curves are essentially curves 1 and 3 in Figs. 6 and 7, and their slopes are equal to C_t or D_tG_s. The soil-water characteristic curve of the silt (Fig. 11) was obtained from the pressure-plate tests. In this plot, the water content was multiplied by the specific gravity G_s for the purpose of plotting the void ratio and water content to the same scale as shown in Fig. 7 (i.e., curve 4). The slope of the curve is equal to D_mG_s.

The shrinkage curve for the compacted silt is shown in Fig. 12 where the water content is multiplied by the specific gravity G_s. The void ratios corresponding to the various water contents in Fig. 11 can now be found using the shrinkage-test relationship from Fig. 12. As a result, the void ratio versus matric suction relationship (i.e., curve 2 in Figs. 6 and 7) can be constructed using Figs. 11 and 12. The slope of the shrinkage curve (i.e., $de/d(wG_s)$ or $[\partial e/\partial(u_a - u_w)]/[\partial(wG_s)/\partial(u_a - u_w)]$) is equivalent to the ratio of volume change indices (i.e., C_m/D_mG_s).

The combined information from Figs. 10–12 is plotted in Fig. 13. Figure 13 illustrates the volume change characteristic of an unsaturated, compacted silt. The volume change

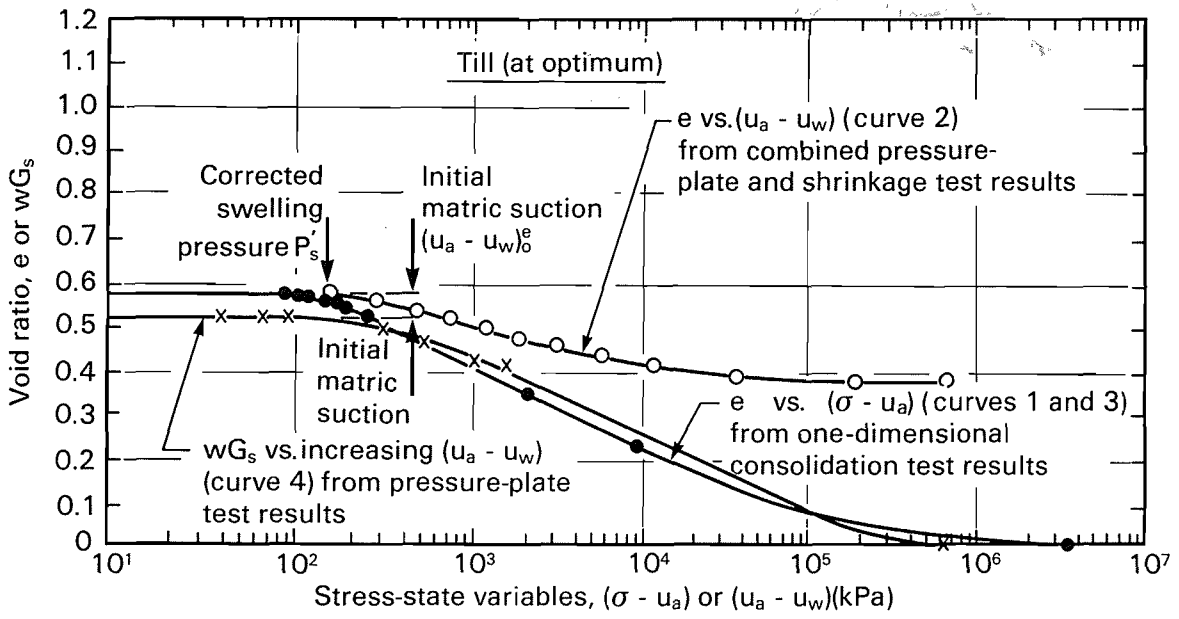

FIG. 18. Volume change relationships for glacial till with optimum water content under one-dimensional loading conditions. Average initial condition: $G_s = 2.76$, $e_0 = 0.567$, $w_0 = 18.7\%$, $w_0G_s = 0.516$.

indices (i.e., C_t, C_m, D_t, and D_m) can be computed from Fig. 13. Changes in void ratio and water content due to an increase in total stress or suction can now be predicted using the computed volume change indices.

The volume change indices for loading are shown in Table 2. Also shown in Table 2 are the volume change indices that are applicable to the limiting suction and net total stress planes (i.e., C_t' and C_m'). These indices are obtained using the graphical procedure illustrated in Figs. 4 and 5. In each case, these limiting condition indices, C_t' and C_m', are somewhat smaller in magnitude than the C_t and C_m indices.

The volume change indices associated with the unloading surface can be obtained from the rebound curve in Fig. 10 and from the free-swell test results in Fig. 14. As a result, the volume change indices associated with the loading and unloading surfaces for the silt specimen have been obtained from several basic soil tests.

The same test procedures were applied to other compacted silt and glacial till specimens. Figure 15 summarizes the results of shrinkage tests on the various compacted specimens. The lower the water content or the degree of saturation, the further away is the distance from the shrinkage test curve to the saturation line. Typical volume change relationships for the compacted silt and the glacial till are presented in Figs. 16–18. The relationships are similar to the one discussed in Fig. 13. The computed volume change indices for the compacted silt and glacial till are tabulated in Table 2.

Application of volume change coefficients and indices

The measured volume change coefficients and indices can be applied to the solution of geotechnical problems involving unsaturated soils. For example, the development of excess pore-air and pore-water pressures during undrained loading can be estimated using a knowledge of the volume change coefficients. Subsequently, the analysis of pore-pressure changes during a transient process (e.g., consolidation) also requires the use of volume change coefficients.

The amount of heave due to the unloading of a soil can be computed using the relevant volume change coefficients for the soil. The analysis for the prediction of heave is done differently for various geographic regions of the world. Some analyses are performed in terms of void ratio change, whereas others are performed in terms of water content changes. Some analyses take the application of total stress changes into account, whereas others only consider changes in matric suction. If any attempt is made to relate the various methods, it is necessary to know the relationship between the various moduli on the constitutive surface for an unsaturated soil. The same reasoning can be applied to the case of settlement predictions for loading a soil.

In the study of the shear strength behavior of unsaturated soils, it is again of interest to know the relationship between changes in void ratio and water content for various applied loads and matric suction values.

Critical state soil mechanics is an area of considerable research in recent years. This area of study involves the presentation of a combination of the shear strength and volume change (and water content) properties of a soil. This means that a complete understanding of the volume change and water content versus stress state variables is an important part of a critical state model for unsaturated soils.

Summary

Oedometer, pressure-plate, and shrinkage tests are the experiments required for measuring the volume change indices corresponding to the loading of an unsaturated soil. These tests can be performed using conventional soil mechanics testing procedures. The test results provide an understanding of the volume change and water content relationships during the loading of an unsaturated soil.

The rebound portion of the oedometer test and the free-swell test are required for determining the volume change indices corresponding to the unloading portion of an unsaturated soil.

Aitchison, G.D., and Martin, R. 1973. A membrane oedometer for complex stress-path studies in expansive clays. Proceedings, 3rd International Conference on Expansive Soils, Haifa, vol. 2, pp. 83–88.

Aitchison, G.D., and Woodburn, J.A. 1969. Soil suction in foundation design. Proceedings, 7th International Conference on Soil Mechanics and Foundation Engineering, Mexico City, vol. 2, pp. 1–8.

ASTM. 1981. Standard test method for capillary-moisture relationships for coarse and medium textured soils by porous plate apparatus. ASTM D2325-68. American Society for Testing and Materials, Philadelphia.

ASTM. 1985*a*. Standard test method for shrinkage factors of soils. ASTM D427. American Society for Testing and Materials, Philadelphia.

ASTM. 1985*b*. Standard test method for one-dimensional consolidation properties of soils. ASTM D2435. American Society for Testing and Materials, Philadelphia.

ASTM. 1985*c*. Standard test method for one-dimensional swell or settlement potential of cohesive soils. ASTM D4546. American Society for Testing and Materials, Philadelphia.

Chen, F.H. 1975. Foundation on expansive soils. 1st ed. Elsevier Science Publishing Co., Inc., New York.

Croney, D., and Coleman, J.D. 1954. Soil structure in relation to soil suction. Journal of Soil Science, **5**: 75–84.

Escario, V. 1969. Swelling of soils in contact with water at a negative pressure. Proceedings, 2nd International Research and Engineering Conference on Expansive Soils. Texas A and M University, College Station, pp. 207–218.

Fredlund, D.G. 1967. Comparison of soil suction and one-dimensional consolidation characteristics of a highly plastic clay. National Research Council of Canada, Division of Building Research, Technical Report 245.

Fredlund, D.G., and Morgenstern, N.R., 1976. Constitutive relations for volume change in unsaturated soils. Canadian Geotechnical Journal, **13**: 261–276.

Gilchrist, H.G. 1963. A study of volume change of a highly plastic clay. M. Sc. Dissertation, University of Saskatchewan, Saskatoon.

Head, K.H. 1984. Manual of soil laboratory testing. Vol. 1. Soil classification and compaction tests. Pentech Press, London.

Ho, D.Y.F. 1988. The relationship between the volumetric deformation moduli of unsaturated soils. Ph.D. thesis, Department of Civil Engineering, University of Saskatchewan, Saskatoon.

Ho, D.Y.F., and Fredlund, D.G. 1989. Laboratory measurement of the volumetric deformation moduli for two unsaturated soils. Proceedings, 42nd Canadian Geotechnical Conference, Winnipeg, Man., Oct. 23–25, pp. 50–60.

Holtz, H.G., and Gibbs, H.J. 1956. Engineering properties of expansive clays. Transactions of the American Society of Civil Engineers, **121**: 641–663.

Lambe, T.H., and Whitman, R.V. 1979. Soil mechanics. John Wiley & Sons Inc., New York.

Lidgren, R.A. 1970. Volume change characteristics of compacted till. M.Sc. dissertation, University of Saskatchewan, Saskatoon.

McWhorter, D.B., and Nelson, J.D. 1979. Unsaturated flow beneath tailings impoundments. ASCE Journal of the Geotechnical Engineering Division, **105**: 1317–1334.

Mitchell, P.H., and Avalle, D.L. 1984. A technique to predict expansive soil movements. Proceedings, 5th International Conference on Expansive Soils, Adelaide, Australia, pp. 124–130.

Noble, C.A. 1966. Swelling measurements and prediction of heave for a lacustrine clay. Canadian Geotechnical Journal, **3**: 32–41.

Rahardjo, H., Ho, D.Y.F., and Fredlund, D.G. 1990. Testing procedures for obtaining volume change indices during loading of an unsaturated soil. Proceedings, 1990 Canadian Society of Civil Engineers Annual Conference, Hamilton, Ont., vol. II-2, May 15–18, pp. 558–573.

Richards, B.G., Peter, P., and Martin, R. 1984. The determination of volume change properties in expansive soils. Proceedings, 5th International Conference on Expansive Soils, Adelaide, Australia, pp. 179–186.

Schmertmann, J.M. 1955. The undisturbed consolidation of clay. Transactions of the American Society of Civil Engineers, **120**: 1201.

Terzaghi, K. 1943. Theoretical soil mechanics. John Wiley & Sons Inc., New York.

Terzaghi, K., and Peck, R.B. 1967. Soil mechanics in engineering practice. John Wiley & Sons Inc., New York.